

Homemade Bread: Repurposing an Ancient Technology for Low Cost *in vitro* Tissue Engineering

Jessica T. Holmes¹, Ziba Jaberansari¹, William Collins¹, Maxime Leblanc Latour¹, Daniel J. Modulevsky² and Andrew E. Pelling^{1,2,3,4*}

¹*Department of Physics, STEM Complex, 150 Louis Pasteur Pvt., University of Ottawa, Ottawa, ON, K1N5N5 Canada*

²*Department of Biology, Gendron Hall, 30 Marie Curie, University of Ottawa, Ottawa, ON, K1N5N5 Canada*

³*Institute for Science Society and Policy, Simard Hall, 60 University, University of Ottawa, Ottawa, ON, K1N5N5 Canada*

⁴*SymbioticA, School of Human Sciences, University of Western Australia, Perth, WA, 6009 Australia*

* Author for correspondence

Andrew E. Pelling; Tel. +1 613 562 5800 Ext 6965; Fax. +1 613 562 5190; Email: a@pellinglab.net

Keywords: Plant-based biomaterials; Bread; Tissue Engineering; Cellular Agriculture;

ABSTRACT

Cellular function is well known to be influenced by the physical cues and architecture of their three dimensional (3D) microenvironment. As such, numerous synthetic and naturally-occurring biomaterials have been developed to provide such architectures to support the proliferation of mammalian cells *in vitro* and *in vivo*. In recent years, our group, and others, have shown that scaffolds derived from plants can be utilized for tissue engineering applications in biomedicine and in the burgeoning cultured meat industry. Such scaffolds are straightforward to prepare, allowing researchers to take advantage of their intrinsic 3D microarchitectures. During the 2020 SARS-CoV-2 pandemic many people around the world began to rediscover the joy of preparing bread at home and as a research group, our members participated in this trend. Having observed the high porosity of the crumb (the internal portion of the bread) we were inspired to investigate whether it might support the proliferation of mammalian cells *in vitro*. Here, we develop and validate a yeast-free “soda bread” that maintains its mechanical stability over two weeks in culture conditions. The scaffolding is highly porous, allowing the 3D proliferation of multiple cell types relevant to both biomedical tissue engineering and the development of novel future foods. Bread derived scaffolds are highly scalable and represent a surprising new alternative to synthetic or animal-derived scaffolds for addressing a diverse variety of tissue engineering challenges.

1. INTRODUCTION

In recent years, there has been an increase in studies on the use of plant-derived biomaterials for tissue engineering applications [1–10]. For example, in work from our group we were able to demonstrate that decellularization of plant tissues resulted in cellulose-rich three dimensional (3D) scaffolds [1–3]. In addition, we have demonstrated that these scaffolds also perform very well after implantation into animal models, resulting in a high degree of tissue integration and vascularization [2,3]. Several other groups have now published similar studies with a multitude of plant tissues and mammalian cell types to demonstrate the general utility of plant-derived biomaterials for biomedical and food-based tissue engineering applications [6–10]. A growing body of literature also suggests that plant-derived proteins can be utilized to create scaffolds for tissue engineering and are broadly compatible with mammalian cell culture. Proteins such as soy, zein and camelina, etc have been studied, but of particular interest are gluten proteins derived from wheat, such as gliadin and glutenin [11–13]. These wheat derived proteins can be purified and made into films suitable to culture mammalian cells. For instance, glutenin films have been demonstrated to be an acceptable substrate for osteoblasts [12]. In the same study, a gluten film was shown to support the growth of osteoblasts but with less efficiency due to the cytotoxicity of gliadin [12]. Wheat protein based scaffolds can also be obtained through electrospinning, in which ultrafine fibrous structures can be obtained, creating a polymer melt film of wheat glutenin [13]. Such scaffolds have been shown to support the culture of adipose derived mesenchymal stem cells [12]. Although effective, these methods are labor and resource intensive, requiring two days to purify the proteins and seven days for them to be electrospun [12,13].

Regardless, the development of naturally derived 3D biomaterials has gained considerable interest in recent years due to their potential for use in biomedical tissue engineering and cellular agriculture applications. Although still emerging, the broader goal of cellular agriculture [14–16] is to replace products produced by traditional agricultural methods with biotechnological approaches such as synthetic biology and tissue engineering [14,15]. One specific focal point within the field is the cultivation of mammalian cells *in vitro* for the preparation of meat-like products [5,14,17]. Although a number of challenges remain to achieve this goal, a significant body of work has begun to address issues such as the large scale production of relevant cell types, creating sustainable and ethically sourced media and developing suitable scaffolds [5,14,15,17]. Plant-derived scaffolds are of particular interest due to the potential of creating edible scaffolds [5] Inspired by the simplicity of plant-based biomaterials, here we investigated the possibility of developing a simple and straightforward approach to fabricating wheat-derived scaffolds for tissue culture.

The work presented here was strongly influenced and motivated by current global events, namely the SARS-CoV-2 pandemic. As many people around the world found themselves physically distancing and working from home, baking bread rapidly gained a large increase in popularity. According to Google Trends, the search queries for the term 'bread' spiked in the early days of the global pandemic [18]. As with many other laboratories around the world, our laboratory was shut down during this same period. As a research group, many of us found that we were also participating in our own efforts to bake bread at home. Sharing our experiences, we hypothesized that baked bread might also possess the structural characteristics to make it suitable as a 3D, porous and biocompatible biomaterial for mammalian cell culture applications. During that time we designed a series of experiments which have since been performed, the results of which we present below. The main ingredient, wheat flour, is primarily composed of starch (~70%) but its strength and stability is mainly attributed to its protein content (~12%), represented by gluten and non-gluten (albumin and globulins) proteins [19]. As described above, such proteins have found potential utility in the creation of biomaterials [11,13].

A requirement for an optimal biomaterial is a structure with high porosity to prevent an anoxic microenvironment. The porous nature of bread results from the presence of a leavening agent, such as yeast or baking powder. The reaction between sodium bicarbonate, the active ingredient in baking powder, and water yields bicarbonate, an anion that decomposes into water and carbon dioxide at ambient temperature and is further favoured when exposed to heat. The carbon dioxide helps the bread rise in addition to leaving behind pores as it exits the crumb. The porous structure of the crumb allows for the migration of cells within the bread which consequently makes it an appealing biomaterial. Moreover, the time required to make the bread is less than an hour, which is highly efficient in comparison to other methods of creating scaffolds for tissue engineering, including plant-based scaffolds. The ingredients needed to make the dough are found in most household pantries and can be purchased at a fraction of the cost of the chemicals often required to fabricate other types of biomaterials.

In this study, we present a bread recipe that can be used as an easily produced scaffold that supports the proliferation of mammalian cells in culture. Our objective was to demonstrate that mammalian cells could remain viable and proliferate *in vitro* within scaffolds made of porous bread crumb. We demonstrate that bread scaffolds remain intact over the course of two weeks in cell culture, can be modified to control their mechanical properties and that mammalian cells will proliferate and remain viable within the scaffolds. Most importantly, the recipe we utilize relies on sodium bicarbonate, rather than yeast, to create the required porosity, thus avoiding potential contamination of the scaffold with an unwanted cell type. The data presented here supports a simple and highly accessible new method for creating cell culture scaffolding utilizing ancient approaches. The inherent porosity of the bread crumb along with its simple production method results in a potentially useful biomaterial that can be utilized for *in vitro* 3D cell culture. Proof-of-concept studies presented here support the use of bread-based scaffolds in biomedical applications of soft tissue, muscle and bone engineering [8,9,20,21]. Much more work will be required to fully elucidate how such a scaffold may be used in these contexts in a clinical setting, if at all, however the results benefit from knowledge gained through previous studies on plant polymers and reveal a novel path forward. Importantly, the growth of the specific cell types studied here support the use of these scaffolds in cellular agriculture applications relating to the development of future foods. As with the biomedical applications of these bread-based scaffolds, more work will be required in order to fully explore the potential use of these biomaterials in this context. Regardless, the research presented here opens a new approach in the development of biomaterials which may ultimately enhance several aspects of human health and well being.

2. MATERIALS AND METHODS

2.1 Bread Recipe and Fabrication

Our approach is based on a common soda bread recipe found widely on the internet. In a ceramic bowl, 120g of all purpose flour (Five Roses), 2g of iodized table salt (Windsor) and 10g of baking powder (Kraft) were mixed together. This was followed by the addition of 70 mL of water, which was heated for 30 seconds in a microwave until the temperature of the water was ~75°C. The mixture was combined to form a dough and shaped into a ball. The dough is then kneaded for 3 minutes with the addition of flour as needed to reduce sticking. Once flattened into a circular disk with a height of approximately 2.5 cm, the dough was placed in a glass bread pan lined with parchment paper. It was baked for 30 minutes at 205°C in a preheated oven. The cooled bread was stored in a resealable plastic bag (Ziploc) at -20°C until use.

When ready for use, the bread was thawed to room temperature. A 6mm biopsy punch is then be used to extract cylindrical samples from the internal portion of the loaf (ie. the “crumb”). The cylinders are then cut with a blade (Leica) to form circular scaffolds, which were about 2.5mm in thickness. Two formulations were tested, the native untreated scaffolds as well as a group of chemically crosslinked scaffolds. To crosslink the samples with glutaraldehyde (GA) we adapted an approach described previously for similar protein based scaffolds [22,23]. A 0.5% GA solution was prepared from a 50% electron microscopy grade glutaraldehyde stock (Sigma) and diluted with PBS (Fisher). The scaffolds were incubated in the GA solution overnight in the fridge. Afterwards, the scaffolds were rinsed 3 times with PBS. To reduce any remaining traces of unreacted glutaraldehyde, the scaffolds were incubated in a 1 mg/mL NaBH₄ (Acros Organics) solution on ice, made immediately before use. Once the formation of bubbles ceased, the samples were rinsed 3 times with PBS.

2.2 Cell Culture

NIH3T3 mouse fibroblasts stably expressing GFP were used in this study (ATCC). Cells were cultured in high glucose Dulbecco's Modified Eagle Medium (DMEM) (HyClone), supplemented with 10% fetal bovine serum (HyClone) and 1% penicillin/streptomycin (HyClone) at 37°C and 5% CO₂. The culture media was exchanged every second day and the cells were passaged at 70 % confluence. To test the suitability of the scaffold to support the proliferation of other cell types, C2C12 mouse myoblasts and MC-3T3 mouse pre-osteoblasts were also cultured on the scaffolds according to the protocols above. In the case of MC-3T3 cells, the DMEM was replaced with Minimum Essential Medium (MEM) (ThermoFisher).

To prepare bread scaffolds for seeding, they were placed in 70% ethanol for 30 minutes in order to sterilize them and then rinsed twice with PBS. Bread scaffolds were additionally soaked in complete media prior to seeding to encourage adherence. A droplet containing 1.0×10⁵ cells was then gently placed on top of each scaffold which were contained in 12-well plates. The samples were placed in the incubator for 3-4 hours to allow the cells to adhere to the scaffolds. Afterwards, 1.5-2 mL of culture media was added to each well and the samples were incubated. The culture media was exchanged every 48-72 hours. Cells were maintained on scaffolds for two weeks in a standard cell culture incubator.

2.3 Staining

Before staining, the scaffolds were fixed in 4% paraformaldehyde for 10-15 minutes. Following 3 rinses with a duration of 5 minutes each in PBS, the samples are stained using a stock DAPI (ThermoFisher) stock solution (1:500 in PBS) for 15 minutes to label nuclei. In cases where C2C12 and MC-3T3 cells were cultured, after fixation with 3.5% paraformaldehyde the cells were permeabilized with Triton X-100 and the actin was labelled with a phalloidin 488 (ThermoFisher) stock solution (1:100 in PBS). After staining, all scaffolds were rinsed for 2 minutes with PBS. The scaffolds were then stained using a 0.2% (m/m) Congo Red (Sigma) stock solution for 15 minutes which was followed by 5-10 minute washes with PBS prior to mounting and imaging.

2.4 Confocal Microscopy

Confocal images were obtained using an A1R high speed laser scanning confocal system on a TiE inverted optical microscope platform (Nikon, Canada) with appropriate laser lines and filter sets. Images were analyzed using ImageJ open access software (<http://rsbweb.nih.gov/ij/>). Brightness and contrast adjustments were the only manipulations performed to images. The ImageJ software was also used to count the number of cells in different areas of the scaffolds.

2.5 Scanning Electron Microscopy

The preparation of the samples for SEM began with a fixation in paraformaldehyde. This was followed by a dehydration through successive washes of ethanol with increasing concentration (35%, 50%, 70%, 95% and 99%). The samples are dried using a critical point dryer and gold-coated at a current of 15 mA for 3 minutes with a Hitachi E-1010 ion sputter device. SEM images were acquired at a voltage of 2.00 kV on a JEOL JSM-7500F FESEM.

2.6 Cell Viability Assay

Cell viability was assessed with the Alamar Blue assay (Invitrogen). Cells were seeded onto scaffolds and assessed after 1 and 13 days in culture. In each case, samples were incubated with 10% (v/v) Alamar blue solution standard culture media for 2h in the incubator. Following incubation, The fluorescence was measured in a microplate reader at 570nm against reference wavelength at 600nm. The results are expressed in arbitrary units (AU) and normalized against the initial readings after 1 day in culture.

2.7 Mechanical Testing

The Young's modulus of the scaffolds was determined by compressing the material to a maximum 20% strain, at a rate of 3 mm/min, using a custom-built mechanical tester controlled with LabVIEW software. The force-compression curves were converted to stress-strain curves and the slope of the linear regime between 10-20% compression was fit to extract the Young's modulus.

2.8 Statistics

For the comparison of time series data, a one way ANOVA with Tukey's post-hoc analysis was used to determine the statistical difference between sample populations. To compare between two distinct populations a student's t-test was employed. In all cases alpha = 0.05. Where indicated, all values are presented as the mean \pm standard deviation. Analysis and statistical tests were conducted using the OriginLab software package.

3. RESULTS

3.1 Preparing sterile bread-derived scaffolds

Scaffolds were fabricated as described in the methods section and in a manner similar to many bread recipes. First dry ingredients were combined followed by mixing in warm water and kneading (Fig. 1a, b). After baking the internal part (crumb) of each loaf was characterized by a network of material which possessed a significant variability in its porosity (Fig. 1c, d). To prepare the bread as a scaffold for supporting cell culture, a 6mm biopsy punch was used to extract a cylinder of material from the internal portion of the loaf, also known as the crumb. The cylinder was then sliced with a scalpel to create approximately 2.5mm thick, 6mm diameter circular pieces of material (Fig. 1d).

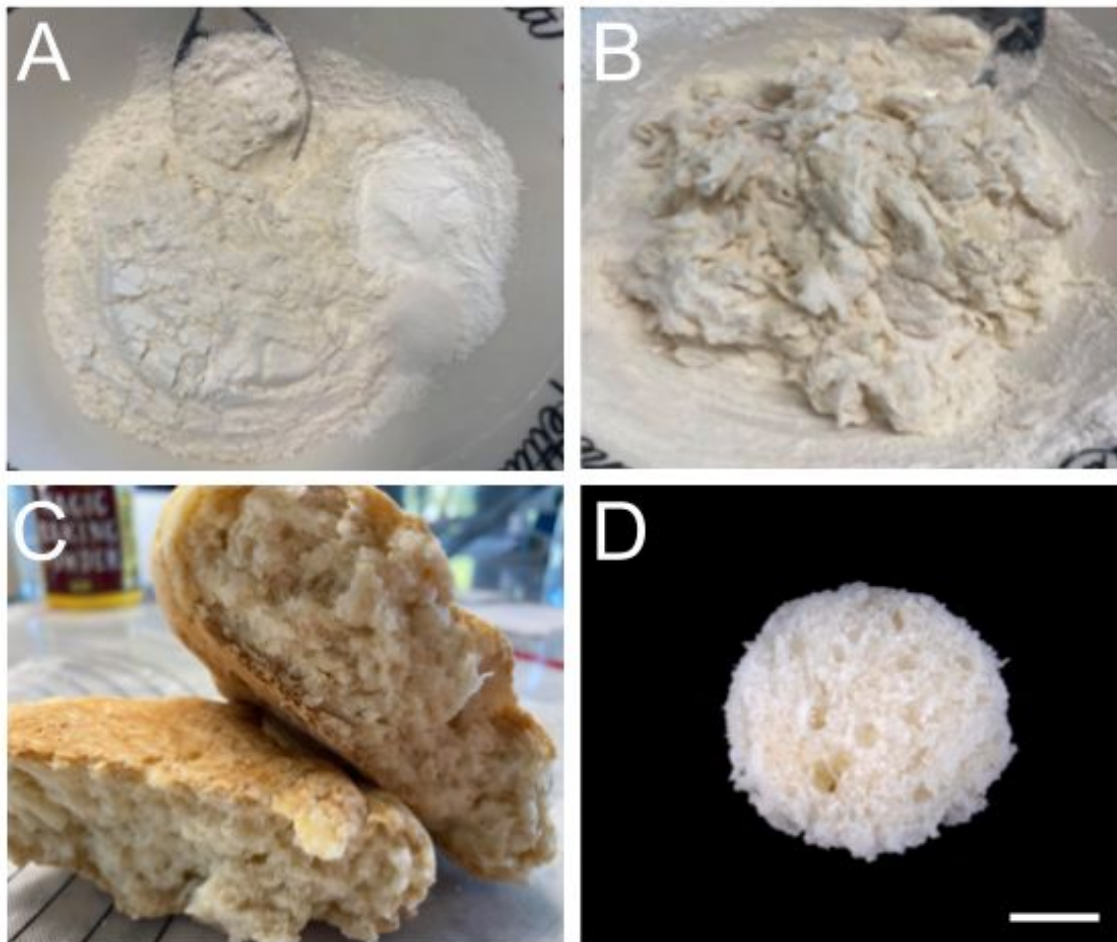


Figure 1. Fabrication of baked bread (BB) scaffolds. A) Dry ingredients (flour, salt, baking powder). B) Assembling the ingredients with warm water creates a dough. C) After baking the dough the bread crumb is utilized for the fabrication of scaffolds for cell culture testing. D) Utilizing a 6mm biopsy punch, 2.5mm thick cylindrical scaffolds can be created from the crumb (scale bar = 2mm). The porous nature of the scaffolds is hypothesized to be sufficient to support mammalian cell culture.

3.2 Mechanical and structural stability of bread-derived scaffolds over time in culture conditions

We designed this study to assess cell proliferation and infiltration over the course of two weeks in culture. This would require the baked bread (BB) scaffolds to be continuously and completely submerged in cell culture media at 37°C for the entire length of time. We were concerned that the native structure of the scaffold may begin to soften significantly and/or decompose over this time course. Therefore, we also created scaffolds that were

glutaraldehyde crosslinked (xBB) to create a more stable structure. The mechanical properties of BB and xBB scaffolds were then measured after initially submerging in cell culture media (Day 1), 24 hr (Day 2) and 288 hr (Day 13) in culture media at 37°C with no mammalian cells (Fig. 2a, b). The results demonstrate that initially, there is no statistically significant difference in Young's modulus between the BB and xBB scaffolds due to the large variability (22.8 ± 9.3 kPa and 30.8 ± 9.9 p=0.06716). However, there is a clear difference in mechanical properties of the BB and xBB scaffolds as a function of time. By Day 13, BB scaffolds are observed to soften significantly to 8.8 ± 3.8 kPa ($p = 4.16854 \times 10^{-6}$) compared to their state on Day 1. In contrast to Day 1, the xBB scaffolds do not soften significantly by Day 13, maintaining a value of 24.2 ± 8.1 kPa ($p = 0.27115$). Although there is a slight downward trend in the xBB scaffolds, it is clearly not as significant as the BB scaffolds. Furthermore, by Day 13, the BB scaffolds are also softer than their xBB counterparts ($p = 2.32518 \times 10^{-6}$). Regardless, in both cases the BB and XBB scaffolds maintain their highly porous morphology and structure after immersion in cell culture media as evidenced by both SEM and confocal imaging (Fig. 2c-f). SEM and confocal imaging reveals that the pore sizes observed in the material can vary significantly over the range of micrometers to millimeters.

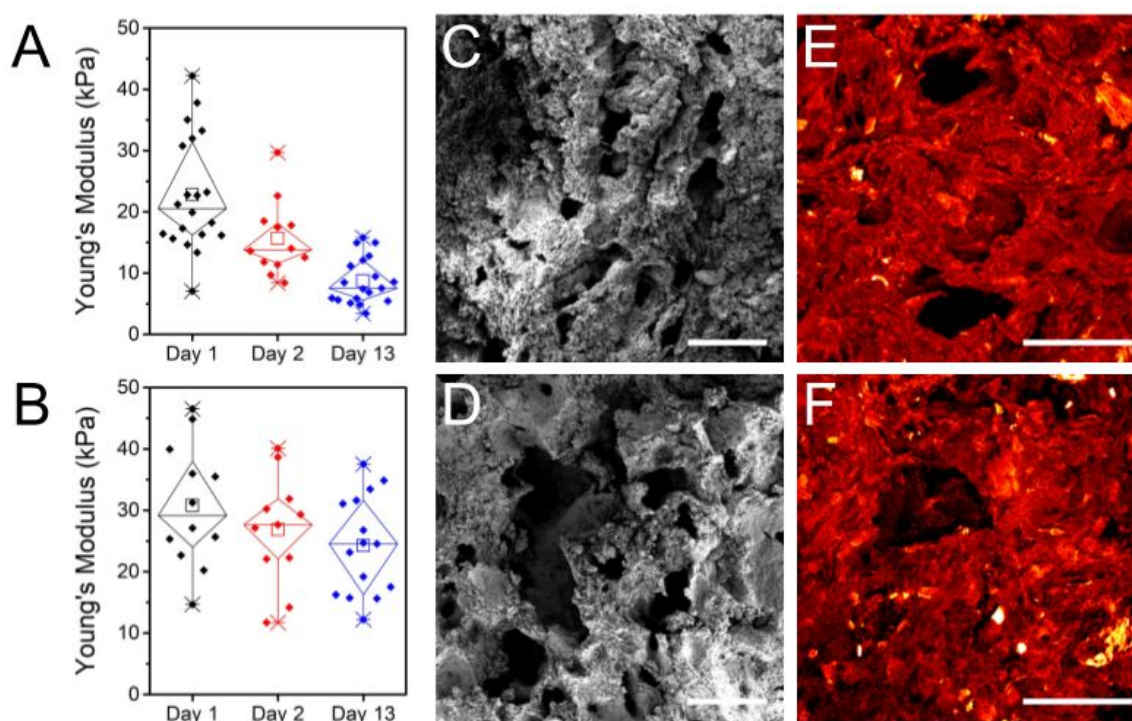


Figure 2. Preliminary analysis of the BB scaffolds after incubation in cell culture media. Mechanical analysis of A) BB and B) xBB scaffolds. Native BB scaffolds soften significantly by Day 13 compared to Day 1 ($p = 4.16854 \times 10^{-6}$). In contrast, the glutaraldehyde cross-linked xBB scaffolds do not exhibit any significant change in mechanical properties by Day 13 compared to Day 1 ($p = 0.27115$). The xBB scaffolds are also significantly stiffer than the BB scaffolds by Day 13 ($p = 2.32518 \times 10^{-6}$). SEM imaging at Day 13 of C) BB and D) xBB scaffolds reveals their porosity is maintained over time under culture conditions (scale bar = 1mm and applies to both). Confocal imaging of congo red stained scaffolds also reveals the presence of pores in E) BB and F) xBB scaffolds (scale bar = 400um and applies to both).

3.2 Cell growth dynamics on BB and XBB scaffolds

Satisfied that the BB and xBB scaffolds were stable over time in cell culture conditions and media, we seeded them with NIH3T3 cells stably expressing GFP to assess cell proliferation. The scaffolds (n=3 at each time point) were subsequently imaged using confocal microscopy at Day 2, 5, 7, 9, 11 and 13. The presence of cells after two days reveals that they adhere to both formulations and tend to initially invade inside of the scaffold pores (Fig. 3a,

b). By Day 13 the cells have clearly proliferated forming a high density of cells (Fig. 3c-f). SEM imaging on the BB scaffold reveals cells covering the surface as well as proliferating inside of the pores (Fig. 3g). For each scaffold formulation (n=3 per time point, per formulation), three randomly chosen 1.3 x 1.3 mm areas were imaged and the total number of cell nuclei were counted in each region and averaged (Fig. 3h). In both cases, the cell density on the scaffolds increases over time and eventually plateaus at about Day 9. The dynamics of cell growth do exhibit some variation during the experimental time course. Initially at Day 2, cell density on the BB and xBB scaffolds is the same ($p = 0.9$) at 548 ± 228 cells/mm² vs 628 ± 428 cells/mm², respectively. However at Day 5, the cell density on the BB scaffolds is significantly higher than the xBB scaffolds at 1682 ± 323 cells/mm² vs 766 ± 260 cells/mm², respectively ($p = 0.008$). While there is some variation in the proceeding time points, there are no statistically significant differences from Day 5 onwards. By Day 13 cell density on the BB and xBB scaffolds is the same at 2308 ± 339 cells/mm² vs 1968 ± 494 cells/mm², respectively ($p = 0.94569$).

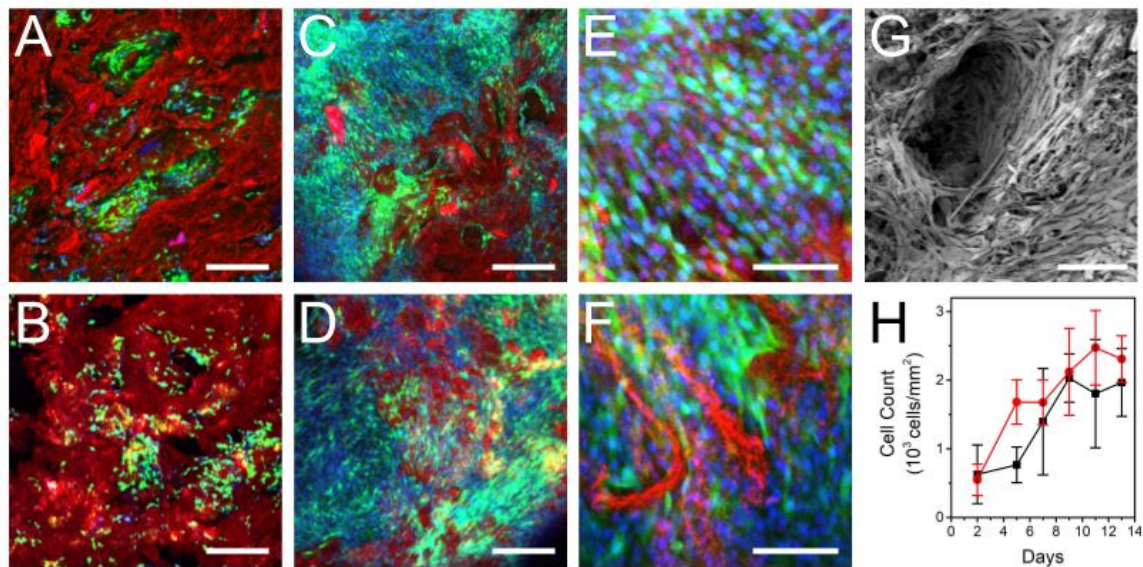


Figure 3. Microscopy and cell proliferation analysis of the BB and xBB scaffolds. On Day 2 after seeding the A) BB and B) xBB scaffolds reveal the presence of a low density of cells which are found on the surface and within cavities of each scaffold (scale bars = 300um). By Day 13 cell density has increased dramatically in C) BB and D) xBB scaffolds, with cells covering most of the available surface (scale bars = 300um). Higher magnification images of the E) BB and F) xBB scaffolds reveals the high density of cells (scale bars = 100um). G) SEM image of cells growing on a BB scaffold reveal how the cells are found inside of the pores of the scaffold as well as on free flat surfaces (scale bar = 100um). Similar results are also observed on xBB scaffolds (data not shown). H) Quantification of cell density on BB (red) and xBB (black) scaffolds reveals similar proliferation dynamics during the experimental time course. There is no significant difference in cell density between the scaffolds except at Day 5 ($p = 0.008$). This indicates that while the cells on the xBB scaffolds exhibit slower proliferation shortly after seeding, they eventually match the growth rate of cells on the BB scaffolds. By Day 13, the cell density on both scaffolds is not significantly different ($p = 0.94569$).

In order to assess the ability of the cells to penetrate into the scaffolds we cross sectioned them as described previously [3]. Briefly, on Day 13, a 6mm diameter, 2.5mm thick xBB cylindrical scaffold was cut longitudinally with a microtome blade to produce two half cylinders. Subsequently, the cut side of the half cylinder could then be washed, fixed and prepared for imaging as described above. The results reveal that cells are indeed able to infiltrate into the deeper portions of the scaffold (Fig. 4). However, as expected the cell density by Day 13 inside the scaffold is much lower than the outer portion [3,4,24]. This phenomenon is commonly observed in many 3D biomaterial scaffolds as it takes time to migrate deeply within a scaffold and due to diminished oxygen/nutrient diffusion the metabolic activity of these cells may be altered compared to cells closer to the exterior portion of the

scaffold. As well, it is difficult to rule out how many cells were sheared off the scaffold surface during the sectioning process. Nevertheless, cells were still clearly observed deeply within the scaffold.

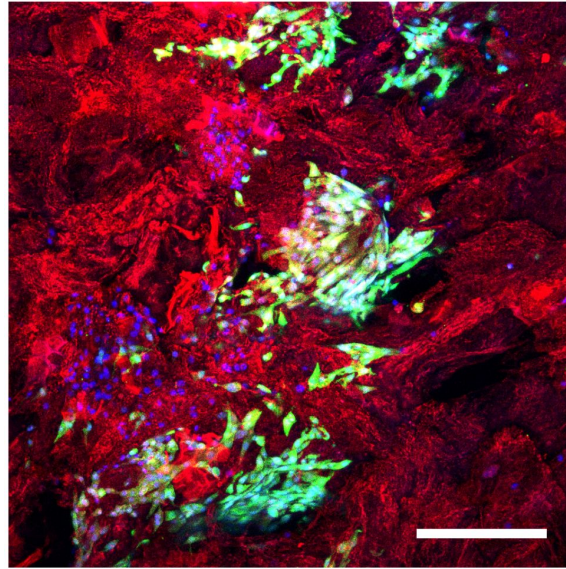


Figure 4. To investigate how deeply cells were able to penetrate into the scaffolds, the cylindrical scaffolds were cut in half to produce two half-cylinders on Day 13. A central region of the internal portion of the scaffold was then imaged. The results reveal that cells are able to penetrate deeply inside of the scaffold (scale bar = 300um). However, consistent with many other 3D biomaterials, cell density was clearly lower than the outer surfaces of the scaffolds when examined at the same point in the experimental time course.

3.3 Metabolic activity of cells proliferating on BB and XBB scaffolds

To assess the viability and metabolic activity of the cells at Day 1 and Day 13 after seeding, we employed the alamar blue assay, which has been successfully used on 3D scaffolds [25] (Fig. 5a). Cell viability was determined by normalizing the measured values against the Day 1 controls to determine a relative fold-increase. For Day 1 and Day 13 BB scaffolds (n=32, n=27, respectively) cell viability increases significantly by a factor of ~4 on average ($p = 4.74779 \times 10^{-10}$). In contrast, on Day 1 and Day 13 xBB scaffolds (n=38, n=36, respectively) cell viability increases by a factor of ~3 on average ($p = 7.50372 \times 10^{-14}$). On both scaffold types the increase in cell viability is significant compared to the initial state. The BB scaffolds do display a large amount of variability in contrast to the xBB scaffolds, however on average there do appear to be more viable cells on these scaffolds ($p = 0.02143$). Further investigation is necessary to clarify why there tend to be slightly more viable cells on the BB scaffolds compared to the xBB scaffolds. This may be due to the high degree of variability or potentially due to changes in surface chemistry of the xBB scaffolds. Regardless, as can be observed in the imaging and cell counting data (Fig. 3), both scaffold types clearly support the rapid and extensive proliferation of these cell types over the course of two weeks.

3.4 BB and XBB scaffolds support the growth of multiple cell types

Finally, to perform an assessment of the generality of these scaffolds for multiple cell types we also cultured C2C12 muscle myoblasts (Fig. 5b) and MC-3T3 pre-osteoblasts (Fig. 5c). These cell types were both chosen as they are established model cell types commonly employed in research for tissue engineered scaffolds. As both cell types do not express GFP we stained the actin cytoskeleton in addition to the scaffold and nuclei. As expected, we were able to observe that both cell types proliferated rapidly and in a manner consistent with the GFP-3T3 cells on both scaffold formulations. In the case of the pre-osteoblasts, the highly porous nature (Fig. 5d)

of the substrate is consistent with various other scaffolds encountered in bone tissue engineering [9]. In these cases, pre-osteoblasts are differentiated into osteoblasts which can mineralize porous 3D microenvironments. This preliminary evidence demonstrates that these scaffolds are likely to be compatible with a multitude of cell types. In this study, our goal was to establish the possibility of utilizing highly available and accessible materials to create scaffolding capable of supporting mammalian cell growth *in vitro*. In a general sense, we demonstrate that it is possible to support the growth of multiple mammalian cell types using the methods presented here. Of course, the scaffolds presented in this study will require further validation before being employed in more specific tissue engineering applications both *in vitro* and *in vivo*.

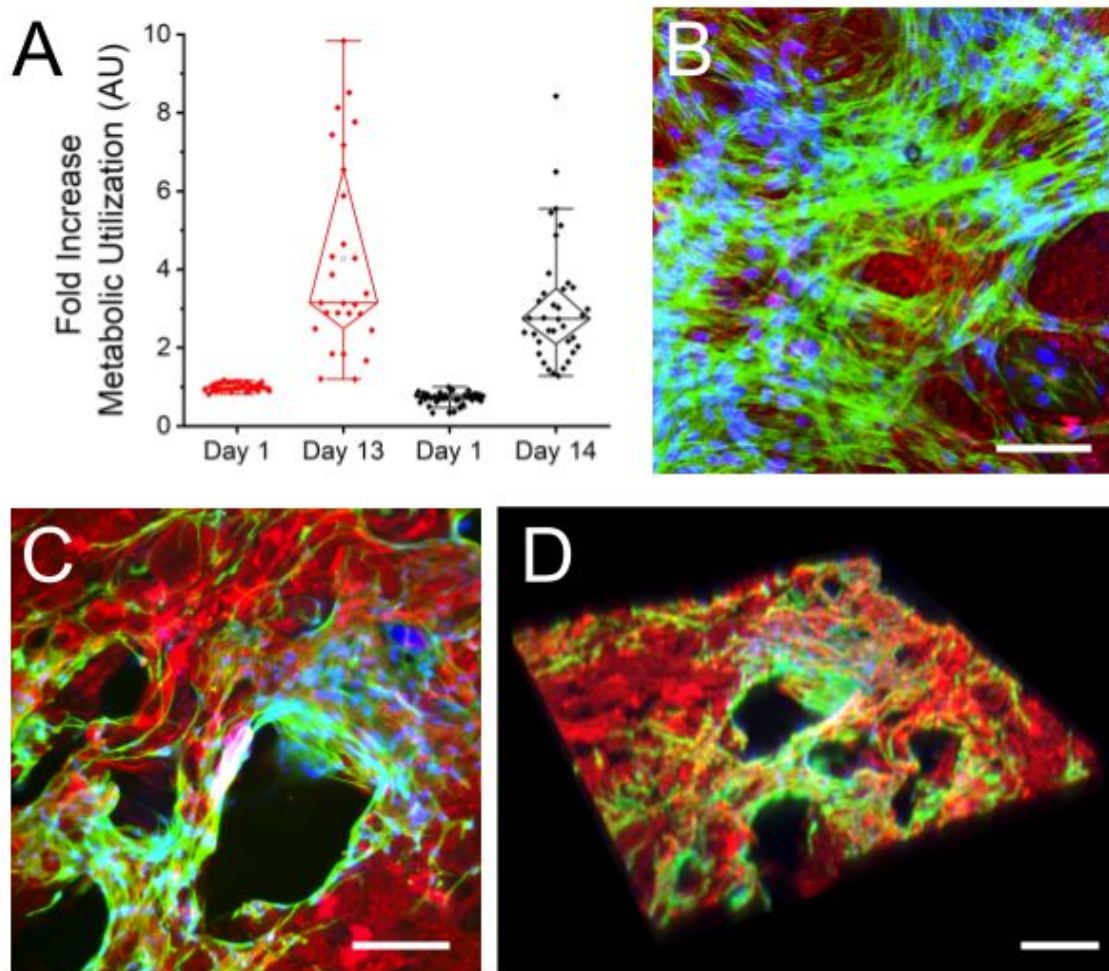


Figure 5. A) Alamar blue assay reveals the relative fold-increase metabolic activity of NIH3T3 fibroblasts after 1 and 13 days of culture on the BB (red) and xBB (black) scaffolds. In both cases, a significant increase in activity is observed by Day 13 compared to the activity after only one day on the scaffold. The data correlates well to the observed increase in cell numbers. In addition, other cell types were also observed to grow on the scaffolds, including B) C2C12 mouse muscle myoblasts, and C) MC-3T3 mouse pre-osteoblasts. D) A 3D reconstruction of a wider field of view of the data in (C) reveals the 3D nature of the scaffold. In the case of MC-3T3 pre-osteoblasts this may be of particular relevance as these cell types are commonly differentiated into bone osteoblasts, normally found in a highly porous microenvironment (scale bar = 50um and applies to all).

4. DISCUSSION

Bread is among one of the oldest foods in human history and its structure, mechanical properties and physicochemical characteristics have been studied extensively [26–29]. However, its applications for tissue engineering have not been explored to our knowledge. Interestingly, the porous architecture of the crumb has been utilized as a sacrificial material to produce scaffolds with potential applications for bone tissue engineering [30]. In this previous example, stale bread was immersed in a slurry of glass powder, which slowly impregnated the crumb. Once fully coated, high temperature thermal treatment removed any organic components, leaving behind a sintered silica-based porous scaffold. Although no direct supporting evidence was presented, the authors did speculate [30] that the mechanical and structural properties of such silica-based scaffolds might have relevance to applications in bone tissue engineering. In contrast, the use of proteins derived from wheat (for example gluten) have been explored extensively in a bioengineering context [11–13]. The viscoelastic properties of gluteins, found in the majority of bread products, impart material properties that are of relevance to tissue engineering applications. As we have shown in our previous work on plant-derived biomaterials, novel scaffolds for tissue engineering applications can be created from unconventional source materials. Although the direct use of plant-derived scaffolds was unusual initially, their inertness and biocompatibility have now been explored by several groups [1–10]. Here, we explore a hypothesis that the porous nature of the crumb in bread might present another opportunity to develop a low cost and accessible scaffolding material which would support the growth of mammalian cells.

As demonstrated above, multiple cell types (fibroblast, myoblast, pre-osteoblast) are able to infiltrate and proliferate throughout the scaffolds over the course of two weeks. Moreover, the use of glutaraldehyde to reinforce the scaffolds (including a subsequent neutralization step to ensure removal of unreacted glutaraldehyde) did not cause any dramatic cytotoxicity as the rate of cell proliferation was similar to the scaffolds that were untreated. In this study, our bread scaffolds are primarily composed of wheat-derived proteins. Specifically, gluten proteins likely impart stability to the scaffolds over time. It does not contain any animal-based products thereby reducing the cost and increasing the simplicity of the recipe. To ensure porosity in our scaffolds, we utilized sodium bicarbonate as the only leavening agent. Although not explored in detail here, the concentration of sodium bicarbonate and/or the use of other compounds may provide a route to further exert control over pore size which was highly variable in our scaffolds.

BB and xBB scaffolds readily absorb liquids and their structural longevity in cell culture media over many days was an immediate concern. Mechanical testing demonstrates a significant decrease in stiffness after the BB scaffolds over time. The increase in softness was addressed by cross-linking the proteins which make up the scaffolds with glutaraldehyde. Once treated, the xBB scaffolds display no significant change in stiffness over time. When comparing the mechanical properties of the BB and xBB scaffolds (which generally vary from 10-30 kPa) with other traditional hydrogel scaffolds, the values tend to fall within the same range [24,31–33]. This leaves open the possibility of employing BB and xBB (or future variants) in a wide range of potential tissue engineering applications [24,33].

SEM and confocal imaging reveals that the BB and xBB scaffolds form porous 3D surfaces and are similar to the multitude of other scaffolding biomaterials that have been developed previously [24]. Both BB and xBB scaffolds support the proliferation of a high density of cells over time and throughout their entire surface. However, alamar blue viability assays did detect a statistically significant drop in the number of viable cells on xBB versus BB scaffolds which was not consistent with image-based cell counting assays. Potential uncertainty in the quantification of cell density from microscopy data may arise due to limitations in imaging depth and penetration inherent in confocal approaches. As well, we suspect the porous nature of the scaffolds likely lead to the washing out of dead cells over the course of two weeks in culture as the media is changed daily [1]. Nonetheless, these limitations arise with any 3D biomaterial under study but regardless, there is a significant amount of cell proliferation occurring on each scaffold over time, in three different cell lines.

Repairing and regenerating damaged or diseased human tissues by utilizing scaffolds to guide cell growth and differentiation is an area under intense development [34,35]. Many remarkable scaffolds have been developed over the decades with applications in soft tissue repair [20], neuroregeneration [36,37], bone tissue engineering [9,21], skin reconstruction [38,39], artificial corneas [40] and skeletal/cardiac muscle regeneration [8,41,42]. A number of approaches in these areas have led to the development of synthetic polymers or animal/insect proteins (collagen, fibronectin, silk, etc) with unique physical, chemical, electrical, optical and mechanical properties specific to each application.

More recently, the science of tissue engineering and biomaterials is being applied to the generation of *in vitro* cultured meat [5,14,17]. This application has unique requirements as the final product must be food safe and edible, which creates additional considerations when developing new scaffolding technologies. Interestingly, the relatively simple bread-based biomaterials presented here may offer a route towards these goals. As the infrastructure to create bread at large scale is already in existence, there is the potential that this supply chain may fit within the broader manufacturing context of lab-grown meat. However, as shown here, the bread scaffolds are significantly more stable after cross-linking. Glutaraldehyde is not necessarily the optimal cross-linker for food-based applications. However, as the scaffolds possess sufficient amounts of protein, well-known enzymes utilized in food processing applications, such as transglutaminase (or other chemical crosslinkers and bread recipes), should be considered as alternatives.

5. CONCLUSIONS

In conclusion, we demonstrate the novel use of an ancient food product as a biomaterial for creating a 3D scaffold to support *in vitro* cell culture. A number of studies utilizing plant proteins and polymers such as soy, zein, gluten, gliadin and cellulose etc [8,11,12] have all shown that they can be used in a variety of tissue engineering applications, though the processing and purification processes they require are more involved than the methods presented in this study. That said, the approaches developed here are highly complementary to previous studies on plant tissues and polymers. While traditional, synthetic biomaterials have often been preferred due to the control over their physicochemical properties, recent evidence has revealed new opportunities made possible with naturally derived biomaterials. Although post-modification methods are typically required to control the architecture, chemical and mechanical properties of such biomaterials, their highly accessible nature and relatively low upfront material cost make them an appealing choice for future biomedical and cellular agriculture applications.

AUTHORSHIP CONTRIBUTION STATEMENT

Jessica T. Holmes: Data curation; Formal analysis; Investigation; Methodology; Roles/Writing - original draft; Writing - review & editing. **Ziba Jaberansari:** Data curation; Investigation; Methodology; Roles/Writing - original draft; Writing - review & editing. **William Collins:** Data curation; Formal analysis; Investigation; Methodology; Roles/Writing - original draft; Writing - review & editing. **Maxime Leblanc Latour:** Data curation; Investigation; Methodology; Roles/Writing - original draft; Writing - review & editing. **Daniel J. Modulevsky:** Data curation; Investigation; Methodology; Roles/Writing - original draft; Writing - review & editing. **Andrew E. Pelling:** Conceptualization; Data curation; Formal analysis; Funding acquisition; Project administration; Resources; Supervision; Roles/Writing - original draft; Writing - review & editing.

DECLARATION OF COMPETING INTEREST

The authors declare that they have no known competing financial interests or personal relationships that could have appeared to influence the work reported in this paper.

ACKNOWLEDGMENTS

This work was supported by grants to Andrew E. Pelling from the National Sciences and Engineering Research Council Discovery Grant, a Canada Research Chair, the Canada Foundation for Innovation and the Li Ka Shing Foundation.

DATA AVAILABILITY

The research data required to reproduce these findings is available upon request from the corresponding author.

REFERENCES

1. Modulevsky DJ, Lefebvre C, Haase K, Al-Rekabi Z, Pelling AE. Apple derived cellulose scaffolds for 3D mammalian cell culture. *PLoS One*. 2014;9: e97835.
2. Modulevsky DJ, Cuerrier CM, Pelling AE. Biocompatibility of Subcutaneously Implanted Plant-Derived Cellulose Biomaterials. *PLoS One*. 2016;11: e0157894.
3. Hickey RJ, Modulevsky DJ, Cuerrier CM, Pelling AE. Customizing the Shape and Microenvironment Biochemistry of Biocompatible Macroscopic Plant-Derived Cellulose Scaffolds. *ACS Biomater Sci Eng*. 2018;4: 3726–3736.
4. Hickey RJ, Pelling AE. Cellulose Biomaterials for Tissue Engineering. *Front Bioeng Biotechnol*. 2019;7: 45.
5. Campuzano S, Pelling AE. Scaffolds for 3D Cell Culture and Cellular Agriculture Applications Derived From Non-animal Sources. *Frontiers in Sustainable Food Systems*. 2019;3: 38.
6. Gershlak JR, Hernandez S, Fontana G, Perreault LR, Hansen KJ, Larson SA, et al. Crossing kingdoms: Using decellularized plants as perfusable tissue engineering scaffolds. *Biomaterials*. 2017;125: 13–22.
7. Jovic TH, Kungwengwe G, Mills AC, Whitaker IS. Plant-Derived Biomaterials: A Review of 3D Bioprinting and Biomedical Applications. *Front Mech Eng Chin*. 2019;5: 19.

8. Cheng Y-W, Shiowski DJ, Ball RL, Whitehead KA, Feinberg AW. Engineering Aligned Skeletal Muscle Tissue Using Decellularized Plant-Derived Scaffolds. *ACS Biomater Sci Eng*. 2020;6: 3046–3054.
9. Lee J, Jung H, Park N, Park S-H, Ju JH. Induced Osteogenesis in Plants Decellularized Scaffolds. *Sci Rep*. 2019;9: 20194.
10. Fontana G, Gershlak J, Adamski M, Lee J-S, Matsumoto S, Le HD, et al. Biofunctionalized Plants as Diverse Biomaterials for Human Cell Culture. *Adv Healthc Mater*. 2017;6. doi:10.1002/adhm.201601225
11. Jahangirian H, Azizi S, Rafiee-Moghaddam R, Baratvand B, Webster TJ. Status of Plant Protein-Based Green Scaffolds for Regenerative Medicine Applications. *Biomolecules*. 2019;9. doi:10.3390/biom9100619
12. Reddy N, Jiang Q, Yang Y. Novel wheat protein films as substrates for tissue engineering. *J Biomater Sci Polym Ed*. 2011;22: 2063–2077.
13. Xu H, Cai S, Sellers A, Yang Y. Electrospun ultrafine fibrous wheat glutenin scaffolds with three-dimensionally random organization and water stability for soft tissue engineering. *J Biotechnol*. 2014;184: 179–186.
14. Stephens N, Di Silvio L, Dunsford I, Ellis M, Glencross A, Sexton A. Bringing cultured meat to market: Technical, socio-political, and regulatory challenges in cellular agriculture. *Trends Food Sci Technol*. 2018;78: 155–166.
15. Stephens N, Sexton AE, Driessen C. Making Sense of Making Meat: Key Moments in the First 20 Years of Tissue Engineering Muscle to Make Food. *Frontiers in Sustainable Food Systems*. 2019;3: 45.
16. Rischer H, Szilvay GR, Oksman-Caldentey K-M. Cellular agriculture — industrial biotechnology for food and materials. *Current Opinion in Biotechnology*. 2020. pp. 128–134. doi:10.1016/j.copbio.2019.12.003
17. K Handral H, Hua Tay S, Wan Chan W, Choudhury D. 3D Printing of cultured meat products. *Crit Rev Food Sci Nutr*. 2020; 1–10.
18. Google Trends. [cited 18 Oct 2020]. Available: <https://trends.google.com/trends/explore?q=bread>
19. Van Der Borght A, Goesaert H, Veraverbeke WS, Delcour JA. Fractionation of wheat and wheat flour into starch and gluten: overview of the main processes and the factors involved. *J Cereal Sci*. 2005;41: 221–237.
20. Sang Y, Li M, Liu J, Yao Y, Ding Z, Wang L, et al. Biomimetic Silk Scaffolds with an Amorphous Structure for Soft Tissue Engineering. *ACS Appl Mater Interfaces*. 2018;10: 9290–9300.
21. Lau CS, Hassanbhai A, Wen F, Wang D, Chanchareonsook N, Goh BT, et al. Evaluation of decellularized tilapia skin as a tissue engineering scaffold. *J Tissue Eng Regen Med*. 2019;13: 1779–1791.
22. Hickey R, Pelling AE. The rotation of mouse myoblast nuclei is dependent on substrate elasticity. *Cytoskeleton*. 2017;74: 184–194.
23. Al-Rekabi Z, Pelling AE. Cross talk between matrix elasticity and mechanical force regulates myoblast traction dynamics. *Phys Biol*. 2013;10: 066003.
24. Abdulghani S, Mitchell GR. Biomaterials for In Situ Tissue Regeneration: A Review. *Biomolecules*. 2019;9. doi:10.3390/biom9110750
25. Brancato V, Kundu B, Oliveira JM, Correlo VM, Reis RL, Kundu SC. Tumor-Stroma Interactions Alter the Sensitivity of Drug in Breast Cancer. 2020. doi:10.3389/fmats.2020.00116

26. Arranz-Otaegui A, Gonzalez Carretero L, Ramsey MN, Fuller DQ, Richter T. Archaeobotanical evidence reveals the origins of bread 14,400 years ago in northeastern Jordan. *Proc Natl Acad Sci U S A*. 2018;115: 7925–7930.
27. Shehzad A, Chiron H, Della Valle G, Kansou K, Ndiaye A, Réguerre AL. Porosity and stability of bread dough during proofing determined by video image analysis for different compositions and mixing conditions. *Food Res Int*. 2010;43: 1999–2005.
28. Gao J, Wang Y, Dong Z, Zhou W. Structural and mechanical characteristics of bread and their impact on oral processing: a review. *Int J Food Sci Technol*. 2018;53: 858–872.
29. Rathnayake HA, Navaratne SB, Navaratne CM. Porous Crumb Structure of Leavened Baked Products. *Int J Food Sci*. 2018;2018: 8187318.
30. Fiume E, Serino G, Bignardi C, Verné E, Baino F. Bread-Derived Bioactive Porous Scaffolds: An Innovative and Sustainable Approach to Bone Tissue Engineering. *Molecules*. 2019;24. doi:10.3390/molecules24162954
31. Saxena S, Hansen CE, Lyon LA. Microgel mechanics in biomaterial design. *Acc Chem Res*. 2014;47: 2426–2434.
32. Engler AJ, Sen S, Sweeney HL, Discher DE. Matrix elasticity directs stem cell lineage specification. *Cell*. 2006;126: 677–689.
33. Wang L, Wang C, Wu S, Fan Y, Li X. Influence of the mechanical properties of biomaterials on degradability, cell behaviors and signaling pathways: current progress and challenges. *Biomater Sci*. 2020;8: 2714–2733.
34. Williams DF. Challenges With the Development of Biomaterials for Sustainable Tissue Engineering. *Front Bioeng Biotechnol*. 2019;7: 127.
35. Shafiee A, Atala A. Tissue Engineering: Toward a New Era of Medicine. *Annu Rev Med*. 2017;68: 29–40.
36. Zhang Q, Nguyen PD, Shi S, Burrell JC, Cullen DK, Le AD. 3D bio-printed scaffold-free nerve constructs with human gingiva-derived mesenchymal stem cells promote rat facial nerve regeneration. *Sci Rep*. 2018;8: 6634.
37. Koffler J, Zhu W, Qu X, Platoshyn O, Dulin JN, Brock J, et al. Biomimetic 3D-printed scaffolds for spinal cord injury repair. *Nat Med*. 2019;25: 263–269.
38. Ansari M, Kordestani SS, Nazralizadeh S, Eslami H. Biodegradable Cell-Seeded Collagen Based Polymer Scaffolds for Wound Healing and Skin Reconstruction. *J Macromol Sci Pt B: Phys*. 2018;57: 100–109.
39. Carvalho T, Guedes G, Sousa FL, Freire CSR, Santos HA. Latest Advances on Bacterial Cellulose-Based Materials for Wound Healing, Delivery Systems, and Tissue Engineering. *Biotechnol J*. 2019;14: e1900059.
40. Ahearne M, Fernández-Pérez J, Masterton S, Madden PW, Bhattacharjee P. Designing Scaffolds for Corneal Regeneration. *Adv Funct Mater*. 2020;102: 1908996.
41. Nakayama KH, Shayan M, Huang NF. Engineering Biomimetic Materials for Skeletal Muscle Repair and Regeneration. *Adv Healthc Mater*. 2019;8: e1801168.
42. Svystonyuk DA, Mewhort HEM, Fedak PWM. Using Acellular Bioactive Extracellular Matrix Scaffolds to Enhance Endogenous Cardiac Repair. *Front Cardiovasc Med*. 2018;5: 35.